nature neuroscience

TrkB phosphorylation by Cdk5 is required for activity-dependent structural plasticity and spatial memory

Kwok-On Lai[1–3], Alan S L Wong[1–3], Man-Chun Cheung[1–3], Pei Xu[1–3], Zhuoyi Liang[1–3], Ka-Chun Lok[1–3], Hui Xie[4], Mary E Palko[5], Wing-Ho Yung[4], Lino Tessarollo[5], Zelda H Cheung[1–3] & Nancy Y Ip[1–3]

The neurotrophin brain-derived neurotrophic factor (BDNF) and its receptor TrkB participate in diverse neuronal functions, including activity-dependent synaptic plasticity that is crucial for learning and memory. On binding to BDNF, TrkB is not only autophosphorylated at tyrosine residues but also undergoes serine phosphorylation at S478 by the serine/threonine kinase cyclin-dependent kinase 5 (Cdk5). However, the *in vivo* function of this serine phosphorylation remains unknown. We generated knock-in mice lacking this serine phosphorylation (*Trkb*$^{S478A/S478A}$ mice) and found that the TrkB phosphorylation–deficient mice displayed impaired spatial memory and compromised hippocampal long-term potentiation (LTP). S478 phosphorylation of TrkB regulates its interaction with the Rac1-specific guanine nucleotide exchange factor TIAM1, leading to activation of Rac1 and phosphorylation of S6 ribosomal protein during activity-dependent dendritic spine remodeling. These findings reveal the importance of Cdk5-mediated S478 phosphorylation of TrkB in activity-dependent structural plasticity, which is crucial for LTP and spatial memory formation.

BDNF and its cognate receptor TrkB are required for multiple aspects of neuronal functions, including neuronal survival and differentiation during development as well as synaptic plasticity of mature neurons[1]. One form of BDNF-dependent synaptic plasticity is hippocampal LTP at the CA3-CA1 synapses, which is widely regarded as a cellular mechanism for learning and memory[2,3]. The induction of LTP in the Schaffer collateral of the hippocampus depends on the NMDA receptor and is associated with dendritic spine remodeling, such as enlargement of spine heads, as well as the formation of new spines[4–6]. Such activity-dependent structural plasticity is believed to underlie persistent changes in synaptic strength during late-phase LTP (L-LTP) and involves both the regulation of actin cytoskeleton and protein synthesis[7,8]. Multiple lines of evidence indicate that the neurotrophin BDNF is important for L-LTP and long-term memory[3]. Synaptic activity increases the secretion and local synthesis of BDNF, and transgenic mice with impaired activity-dependent release and synthesis of BDNF show defects in both L-LTP and long-term memory[9–11]. BDNF promotes the formation and maturation of dendritic spines[12,13], and endogenous BDNF is required for NMDA receptor–induced cytoskeletal changes and dendritic spine remodeling during LTP[8,14]. These findings suggest that the structural plasticity elicited by BDNF following NMDA receptor activation is crucial for L-LTP and long-term memory.

BDNF regulates synaptic function via activation of the receptor tyrosine kinase (RTK) TrkB. Mice lacking TrkB or harboring a mutation (Y816F) in the intracellular domain of TrkB exhibit defects in LTP and hippocampus-dependent learning[15,16]. In addition, the surface expression and synaptic localization of TrkB can be regulated by synaptic activity, which might explain the synapse specificity of BDNF in modulating synaptic strength[3]. Similar to other conventional RTKs, the signaling capability of TrkB depends on ligand-dependent autophosphorylation of tyrosine residues in the intracellular domain. In addition, we have previously reported that BDNF also unexpectedly triggers serine phosphorylation of TrkB in the juxtamembrane region at S478 by the proline-directed serine/threonine kinase Cdk5 (ref. 17). Overexpression of a TrkB construct that lacks the Cdk5 phosphorylation site inhibits neurite outgrowth of cultured hippocampal neurons in response to BDNF, suggesting that serine phosphorylation might be crucial for TrkB signaling *in vitro*. Nonetheless, the physiological importance of this serine phosphorylation of TrkB remains largely unknown.

To understand the *in vivo* function of S478 phosphorylation of TrkB, we generated phosphorylation-deficient knock-in mice (*Trkb*$^{S478A/S478A}$ mice). Here we report that TrkB was phosphorylated at S478 at neuronal synapses, and this phosphorylation was essential for glutamate-induced structural remodeling of dendritic spines as well as hippocampal LTP and spatial memory. Furthermore, we found that S478 phosphorylation was required for the interaction of TrkB with the Rac-specific guanine nucleotide exchange factor (GEF) TIAM1, leading to activation of Rac1 and phosphorylation of S6 ribosomal protein essential for spine morphogenesis. Our results suggest that Cdk5-mediated serine phosphorylation of TrkB regulates NMDA receptor–dependent actin dynamics and protein synthesis via signaling to TIAM1, which is essential for spine remodeling during long-term synaptic plasticity and memory formation. Notably, emerging evidence supports a crucial role for Cdk5 in different

[1]Division of Life Science, The Hong Kong University of Science and Technology, Hong Kong, China. [2]Molecular Neuroscience Center, The Hong Kong University of Science and Technology, Hong Kong, China. [3]State Key Laboratory of Molecular Neuroscience, The Hong Kong University of Science and Technology, Hong Kong, China. [4]School of Biomedical Science, The Chinese University of Hong Kong, Hong Kong, China. [5]Neural Development Section, Mouse Cancer Genetics Program, Center for Cancer Research, National Cancer Institute, Frederick, Maryland, USA. Correspondence should be addressed to N.Y.I. (boip@ust.hk).

Received 5 July; accepted 13 September; published online 14 October 2012; doi:10.1038/nn.3237

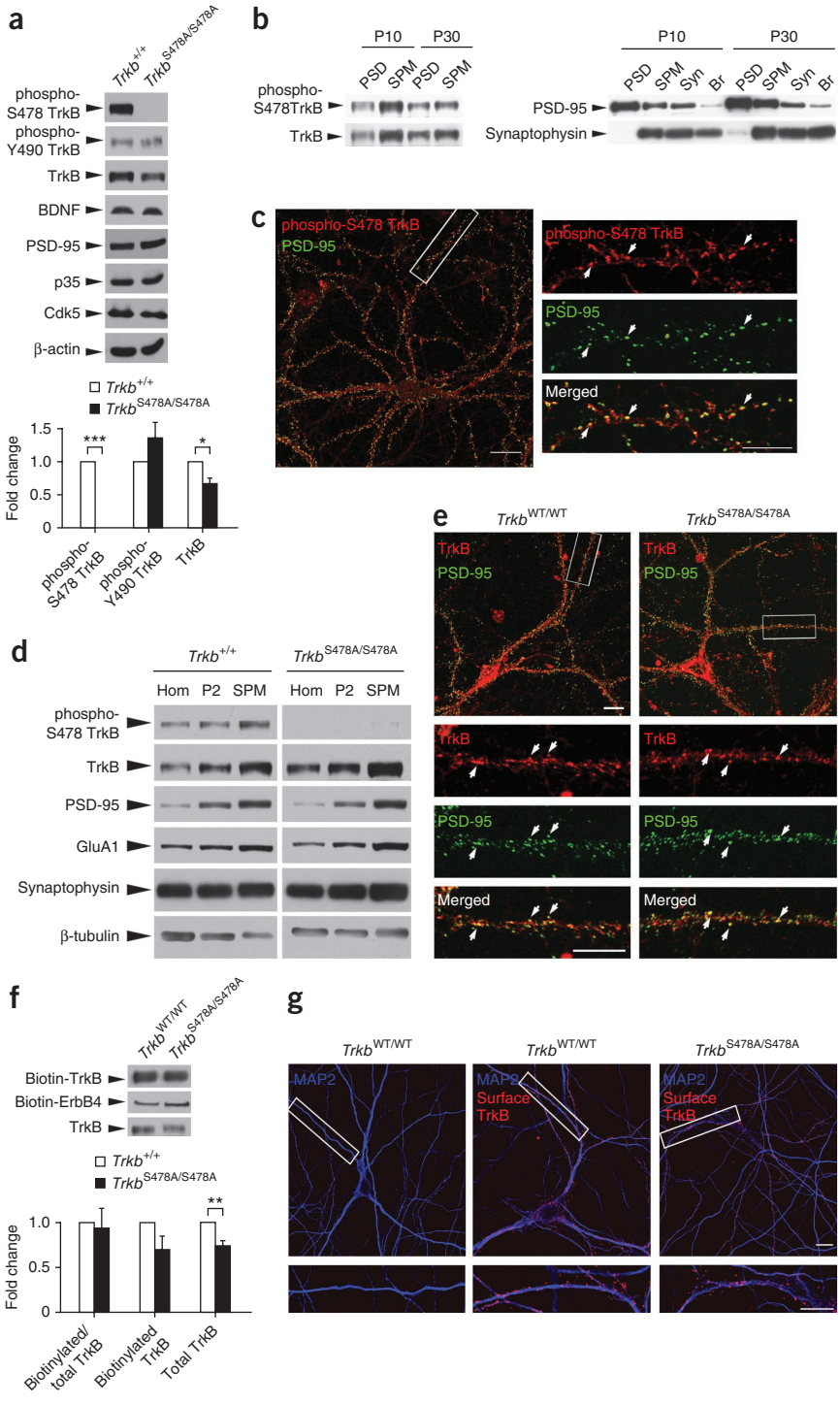

Figure 1 TrkB is phosphorylated at S478 at neuronal synapse. (**a**) Western blotting confirmed that S478 phosphorylation was absent in the brains of *Trkb*$^{S478A/S478A}$ mice. TrkB phosphorylation at Y490 was similar between wild-type (*Trkb*$^{+/+}$) and *Trkb*$^{S478A/S478A}$ mice, although TrkB expression was slightly reduced in *Trkb*$^{S478A/S478A}$ brains. Data are expressed as mean ± s.e.m. and were pooled from three experiments (three pairs of mice for each genotype; $*P < 0.05$, $***P < 0.001$, Student's *t*-test). Full-length blots were presented in **Supplementary Figure 11**. (**b**) TrkB was phosphorylated at S478 in SPM and PSD fractions of rat brains. Enrichment of specific pre- and postsynaptic proteins in the SPM and PSD fractions was verified by antibodies to synaptophysin and PSD-95. (**c**) Colocalization of phospho-S478 TrkB immunoreactivity with the synaptic marker PSD-95 (arrows) in cultured hippocampal neurons. (**d**) TrkB was concentrated in the SPM fraction in both wild-type and *Trkb*$^{S478A/S478A}$ brains. Similar enrichment of TrkB was observed from two different wild-type and *Trkb*$^{S478A/S478A}$ brains. (**e**) Immunofluorescence staining of dissociated hippocampal neurons showed similar colocalization of total TrkB (red) with PSD-95 (green) in *Trkb*$^{WT/WT}$ and *Trkb*$^{S478A/S478A}$ neurons. (**f**) Biotinylation of cultured cortical neurons revealed similar levels of surface TrkB expression (normalized with total TrkB in whole cell lysate) in both *Trkb*$^{WT/WT}$ and *Trkb*$^{S478A/S478A}$ neurons (data are expressed as mean ± s.e.m. and were pooled from three experiments; $P > 0.05$, Student's *t*-test; difference in total TrkB level between *Trkb*$^{WT/WT}$ and *Trkb*$^{S478A/S478A}$ neurons was significant; $**P < 0.01$, Student's *t*-test). (**g**) Surface staining with antibody to the extracellular domain of TrkB showed distinct puncta of surface TrkB (red) in the dendrites (blue) of *Trkb*$^{WT/WT}$ and *Trkb*$^{S478A/S478A}$ neurons (middle and right). The specificity of the surface staining was verified by the absence of red puncta without TrkB antibody (left). Scale bars represent 10 μm.

forms of synaptic plasticity in mature neurons[18]. Knockout mice that lack Cdk5 or its activator p35, as well as transgenic mice with enhanced Cdk5 activity, display altered synaptic plasticity and formation of hippocampus-dependent spatial memory. Our findings therefore reveal a previously unknown cross-talk between BDNF-TrkB signaling and Cdk5, in which TrkB S478 phosphorylation by Cdk5 is critical for NMDA receptor–dependent structural and functional plasticity that underlies spatial memory formation.

RESULTS

Characterization of *Trkb*$^{S478A/S478A}$ knock-in mice

To address the physiological role of TrkB S478 phosphorylation, we generated knock-in mice in which S478 of TrkB is replaced by alanine, and the expression of the transgene was under control of the endogenous *Trkb* (also known as *Ntrk2*) promoter (**Supplementary Fig. 1**). We confirmed homologous recombination of the targeting vector into the mouse embryonic stem cell genome by Southern blot analysis. Heterozygous *Trkb*$^{+/S478A}$ mice were intercrossed to generate wild-type (*Trkb*$^{+/+}$) and *Trkb*$^{S478A/S478A}$ homozygous offspring. A control mutant mouse line (*Trkb*$^{WT/WT}$), with only the *loxP-PGK-neo-loxP* cassette and without the S478A mutation, was also generated in parallel to ensure that the genetic manipulation did not affect splicing and subsequent *Trkb* gene expression. The complete absence of S478 phosphorylation in the *Trkb*$^{S478A/S478A}$ homozygous knock-in mice was confirmed by western blot analysis using antibody that specifically recognized

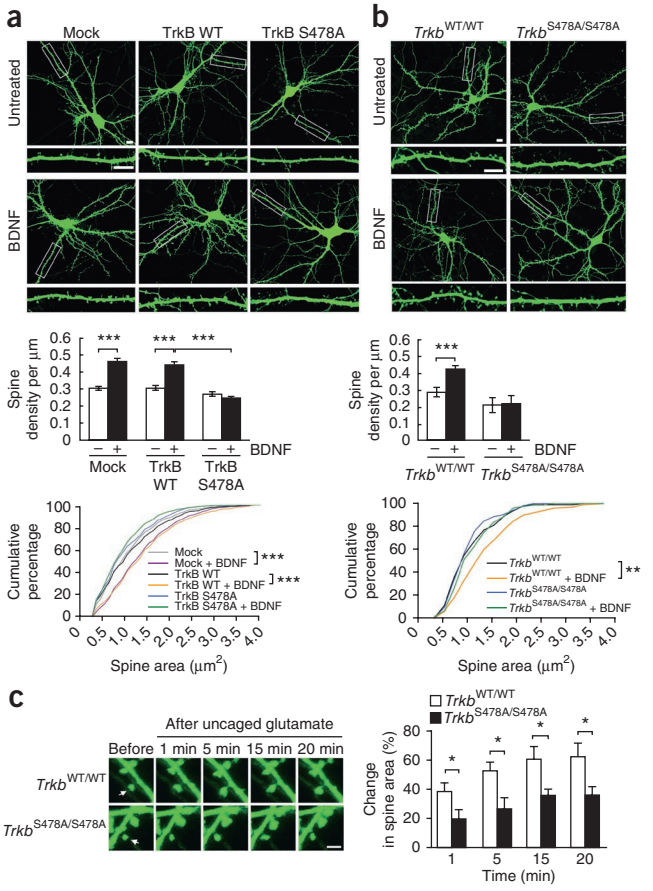

Figure 2 S478 phosphorylation of TrkB is required for BDNF-induced spine morphogenesis and glutamate-induced spine enlargement. (**a**) Hippocampal neurons were co-transfected with GFP and vector (mock), wild-type TrkB (WT), or TrkB S478A construct. Neurons were treated with BDNF for 24 h. Representative images are shown. BDNF increased the spine density (middle; $***P < 0.001$, Student's *t* test) and spine area (bottom; $***P < 0.001$, Kolmogorov-Smirnov test) in mock or wild-type TrkB–expressing neurons, but not in neurons that overexpressed the TrkB S478A mutant. We measured 36 dendrites from 12 neurons for each condition. Scale bars represent 10 µm. (**b**) GFP-transfected hippocampal neurons derived from control (*Trkb*$^{WT/WT}$) or *Trkb*$^{S478A/S478A}$ mice were treated with BDNF for 24 h. Representative images are shown. Treatment with BDNF significantly increased the spine density of the control neurons, but not that of neurons lacking TrkB S478 phosphorylation (middle, 9–16 dendrites from 5–10 neurons were measured for each condition; $***P < 0.001$, one-way ANOVA, Bonferroni's multiple comparison test). BDNF also increased the spine area in control neurons, but not in *Trkb*$^{S478A/S478A}$ neurons (bottom; $**P < 0.01$, Kolmogorov-Smirnov test). Scale bars represent 10 µm. (**c**) GFP-transfected hippocampal neurons (17–18 d *in vitro* (DIV)) cultured from *Trkb*$^{WT/WT}$ or *Trkb*$^{S478A/S478A}$ mutant mice were stimulated by uncaging MNI-glutamate, and the changes in spine size at different duration after glutamate receptor activation were monitored by time-lapse confocal microscopy. Representative images are shown (left). Quantification revealed a significant difference in the fold change in spine area between *Trkb*$^{WT/WT}$ and *Trkb*$^{S478A/S478A}$ neurons in response to uncaged glutamate (right; data were pooled from three experiments, 20 neurons were measured for each genotype; $*P < 0.05$, Student's *t*-test). Scale bar represents 5 µm. Data are expressed as mean ± s.e.m. for the histograms in **a**–**c**.

phospho-S478 TrkB (**Fig. 1a**). TrkB expression was slightly reduced in the knock-in mice (~20%, $P < 0.05$, Student's *t*-test), whereas tyrosine phosphorylation of TrkB was similar to that of wild-type mice ($P > 0.05$, Student's *t*-test).

We then asked whether the subcellular localization of TrkB is affected in the phospho-S478–deficient mutant mice. TrkB is synaptically localized and regulates diverse synaptic functions, such as spine formation and remodeling, trafficking of synaptic proteins and dendritic protein synthesis. We therefore examined whether S478 of TrkB is phosphorylated at synapses. Postsynaptic density (PSD) and synaptic plasma membrane (SPM) fractions were isolated from adult rat brain, and western blotting was performed using antibody to phospho-S478 TrkB (specificity of the antibody was verified using *Trkb*$^{S478A/S478A}$ brain homogenate; **Fig. 1a**). Prominent phospho-S478 TrkB was detected in both the PSD and SPM fractions (**Fig. 1b**). The phosphorylation of TrkB at neuronal synapses was verified by immunofluorescence staining of dissociated hippocampal neurons (**Fig. 1c** and **Supplementary Fig. 2**). However, the synaptic localization of TrkB was not affected in the *Trkb*$^{S478A/S478A}$ knock-in mice (**Fig. 1d**,**e**). Moreover, biotinylation and TrkB surface staining revealed that the phospho-deficient TrkB could be targeted to the plasma membrane (**Fig. 1f**,**g**). Taken together, our data suggest that the lack of S478 phosphorylation does not grossly affect the expression, tyrosine phosphorylation (and hence kinase activity) and localization of TrkB in the *Trkb*$^{S478A/S478A}$ mutant mice.

BDNF-TrkB signaling has been implicated in various aspects of neural development, such as neuronal survival, dendritic growth and spine formation, and TrkB knockout mice die soon after birth. However, the *Trkb*$^{S478A/S478A}$ homozygous knock-in mice were both viable and fertile and did not show gross pathologies or developmental defects. There was no substantial difference in lifespan or body weight between the wild-type and knock-in mice. We also examined the hippocampus morphology and did not observe notable abnormalities in the *Trkb*$^{S478A/S478A}$ mice (**Supplementary Fig. 3a**). In addition, there was no significant difference ($P > 0.05$) in the dendritic arborization and spine development of *Trkb*$^{S478A/S478A}$ neurons both *in vitro* and *in vivo* (**Supplementary Fig. 3b**–**d**). The lack of developmental defects in the *Trkb*$^{S478A/S478A}$ mutant mice suggests that serine phosphorylation does not affect the general signaling capability of TrkB but instead might be involved in specific signaling pathways downstream of the receptor. In particular, the observation that TrkB was phosphorylated at neuronal synapses prompted us to examine whether S478 phosphorylation might regulate the synaptic function of TrkB in the adult brain.

Role of TrkB S478 phosphorylation in spine remodeling

One mechanism by which BDNF modulates synaptic transmission in mature neurons is the regulation of dendritic spine growth and remodeling. To address the role of TrkB S478 phosphorylation, we examined whether Cdk5, which phosphorylates TrkB at S478, is required for BDNF-induced spine morphogenesis. Cultured hippocampal neurons were transfected with GFP at 9 d *in vitro* (DIV) and treated with BDNF for 24 h at 13 DIV. Consistent with previous findings[13], BDNF treatment significantly increased ($P < 0.001$) the density and area of dendritic spines without changing the spine length (**Supplementary Fig. 4a**,**f**). Pharmacological inhibition of Cdk5 by roscovitine or absence of the Cdk5 activator p35 completely abolished the BDNF-induced spine formation and enlargement (**Supplementary Fig. 4b**–**e**). We then asked whether the role of Cdk5 is specifically attributed to the serine phosphorylation of TrkB by co-transfecting hippocampal neurons with GFP and either the wild-type or S478A TrkB mutant construct, followed by treatment with BDNF. Overexpression of the phosphorylation-deficient TrkB construct,

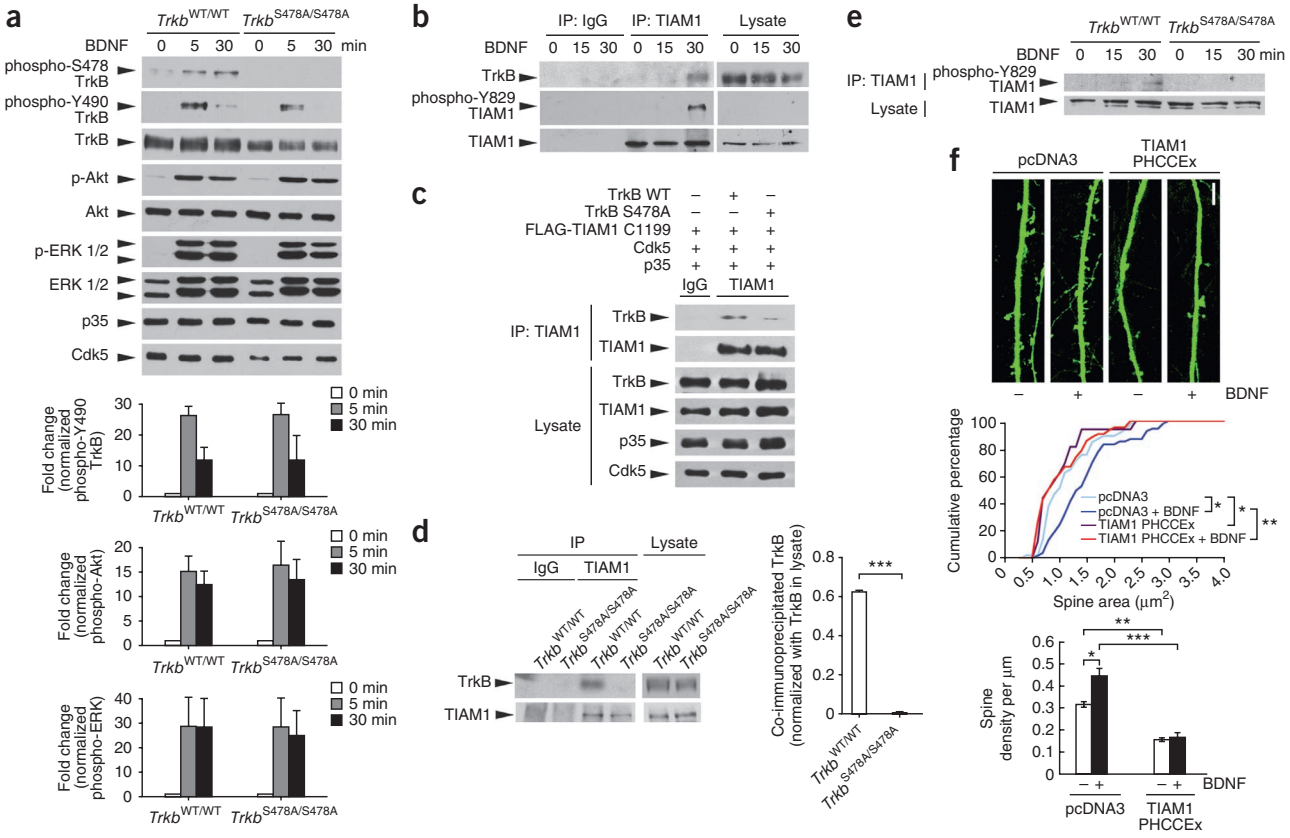

Figure 3 S478 phosphorylation regulates the interaction between TrkB and the Rac GEF TIAM1. (**a**) BDNF-induced TrkB tyrosine phosphorylation and phosphorylation of downstream targets such as AKT and ERK was not affected in *Trkb*$^{S478A/S478A}$ cortical neurons (data were pooled from three experiments with neurons cultured from three mice for each genotype; $P > 0.05$ between *Trkb*$^{WT/WT}$ and *Trkb*$^{S478A/S478A}$ neurons, one-way ANOVA, Bonferroni's multiple comparison test). Full-length blots were presented in **Supplementary Figure 11**. (**b**) BDNF induced tyrosine phosphorylation of TIAM1 and co-immunoprecipitation of TrkB and TIAM1 in cultured cortical neurons. The specificity of the co-immunoprecipitation was confirmed by absence of TrkB and phospho-Y829 TIAM1 in the control immunoprecipitation with IgG. (**c**) Co-immunoprecipitation between TrkB and TIAM1 was performed in 293T cells that overexpressed Cdk5 and p35 together with either wild-type TrkB or TrkB S478A mutant. Mutation of TrkB at S478 substantially reduced its association with TIAM1. (**d**) TIAM1 was co-immunoprecipitated with TrkB in whole-brain lysate from control mice (*Trkb*$^{WT/WT}$), but not the *Trkb*$^{S478A/S478A}$ mice (three pairs of mice for each genotype; $***P < 0.001$, Student's *t*-test). Immunoprecipitation with IgG served as a control for the specificity of interaction. (**e**) Treatment of cortical neurons with BDNF triggered tyrosine phosphorylation of TIAM1 at Y829 in cortical neurons derived from control mice (*Trkb*$^{WT/WT}$), but the induction was completely abolished in *Trkb*$^{S478A/S478A}$ cortical neurons. (**f**) TIAM1 is required for BDNF-induced spine morphogenesis. Coexpression of dominant-negative TIAM1 (TIAM1 PHCCEx) with GFP significantly reduced the area ($*P < 0.05$, Kolmogorov-Smirnov test) and density ($*P < 0.05$, $**P < 0.01$, $***P < 0.001$, one-way ANOVA, Bonferroni multiple comparison test) of dendritic spines before and after BDNF treatment. We measured 21–35 dendrites from 13–19 neurons for each condition. Scale bar represents 10 μm. Data are expressed as mean ± s.e.m. in the histograms of **a**, **d** and **f**.

but not the wild-type TrkB, abolished the effect of BDNF on both spine formation and spine enlargement (**Fig. 2a**). The importance of S478 phosphorylation of TrkB was verified by culturing hippocampal neurons from *Trkb*$^{WT/WT}$ control mice and *Trkb*$^{S478A/S478A}$ mutant mice. Without exogenous BDNF, spine density and size were similar in wild-type and *Trkb*$^{S478A/S478A}$ neurons. However, BDNF treatment increased spine density and area only in wild-type neurons (**Fig. 2b**). These results strongly indicate that S478 phosphorylation of TrkB by Cdk5 is essential for mediating the growth and remodeling of dendritic spines in response to BDNF.

One of the best-studied forms of activity-dependent structural plasticity involves the enlargement of spine heads, which is BDNF-dependent and correlated with enhanced AMPA receptor expression and increase in synaptic strength[8,19]. Given that S478 phosphorylation of TrkB was crucial for BDNF-induced spine enlargement, we asked whether S478 phosphorylation is also involved in activity-dependent spine remodeling. To this end, we used photolysis of MNI-glutamate to examine activity-dependent spine enlargement of dissociated hippocampal neurons using time-lapse confocal microscopy. Uncaging glutamate has been used to induce NMDA receptor–dependent spine remodeling in both hippocampal slices and dissociated hippocampal neurons[6,20,21]. In our study, dissociated hippocampal neurons were transfected with GFP, and selected spines were imaged at real time before and after glutamate uncaging. After a brief 405-nm laser stimulation, we observed a rapid increase in spine size, and the increase was absent without MNI-glutamate (**Supplementary Fig. 5**), indicating that the spine enlargement was triggered by the photolysis of MNI-glutamate instead of a nonspecific side effect of laser illumination. Next, we examined and compared the effect of glutamate uncaging on the increase in spine area between hippocampal neurons cultured from either *Trkb*$^{WT/WT}$ or *Trkb*$^{S478A/S478A}$ mice. Compared with that of control neurons, the magnitude of the increase in spine area after glutamate uncaging was significantly attenuated ($P < 0.05$) in the *Trkb*^{S478A} neurons

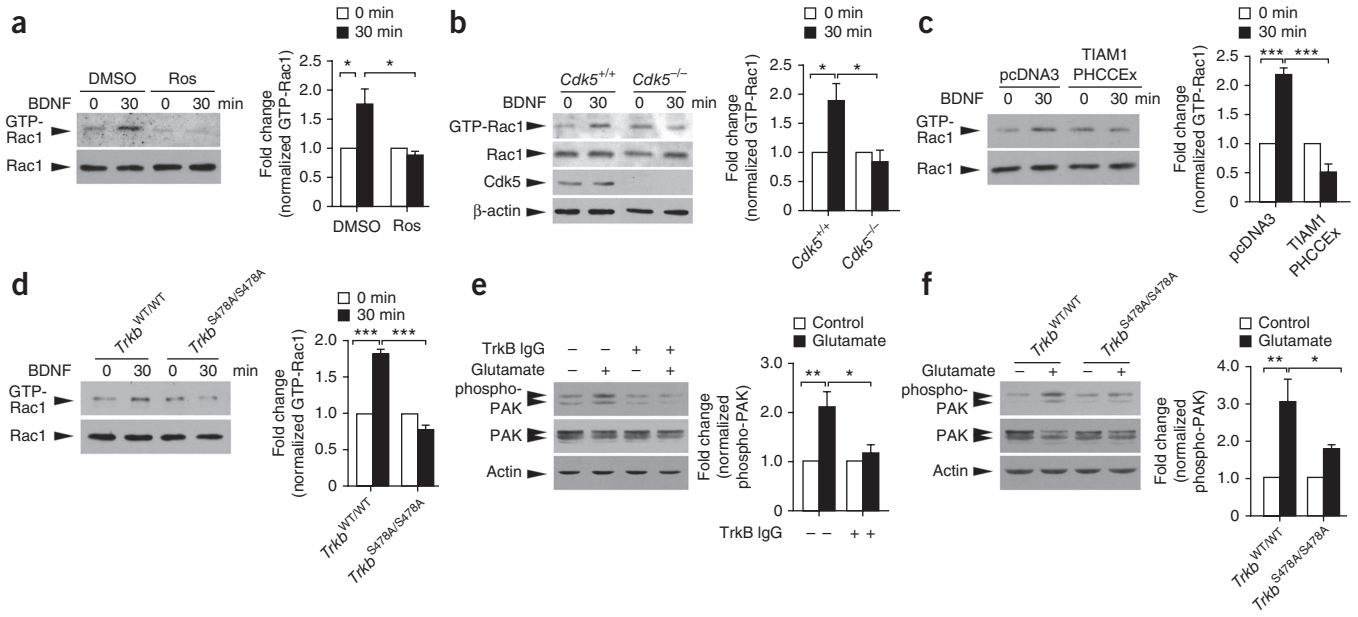

Figure 4 Cdk5-mediated phosphorylation of TrkB at S478 is required for BDNF-induced Rac1 activity and glutamate-induced PAK phosphorylation. (**a**) BDNF induced Rac1 activity in cultured cortical neurons, as indicated by an increase in GTP-bound Rac1. The induction of Rac1 activity by BDNF was abolished in the presence of roscovitine. (**b**) The induction of Rac1 activity by BDNF was abolished in *Cdk5*$^{-/-}$ cortical neurons. (**c**) The enhanced Rac1 activity after BDNF stimulation was blocked in neurons expressing dominant-negative TIAM1. (**d**) BDNF-induced Rac1 activity was abolished in cortical neurons derived from *Trkb*$^{S478A/S478A}$ mice (data were pooled from three experiments for **a**–**c** and four experiments for **d**; $^{*}P < 0.05$, $^{***}P < 0.001$, one-way ANOVA, Bonferroni's multiple comparison test). (**e**) Cortical neurons (14 DIV) were silenced for 4 h by tetrodotoxin and NBQX before treatment with glutamate (50 μM) for 5 min. Glutamate increased phosphorylation of PAK in cortical neurons ($^{**}P < 0.01$), and the increase was significantly attenuated in the presence of TrkB-IgG (1 μg ml^{-1}) (pooled from three experiments, $^{*}P < 0.05$, one-way ANOVA, Tukey multiple comparison test). (**f**) The induction of PAK phosphorylation by glutamate was observed in cortical neurons derived from the control mice *Trkb*$^{WT/WT}$, but the increase in PAK phosphorylation was significantly reduced in *Trkb*$^{S478A/S478A}$ mutant cortical neurons (data were pooled from three experiments, with neurons cultured from three mice for each genotype; $^{*}P < 0.05$, $^{**}P < 0.01$, one-way ANOVA, Tukey multiple comparison test). Data were expressed as mean ± s.e.m. Full-length blots were presented in **Supplementary Figure 11**.

(**Fig. 2c**), supporting the notion that S478 phosphorylation of TrkB is involved in activity-dependent spine remodeling.

TrkB interaction with TIAM1 requires S478 phosphorylation

To investigate the molecular mechanisms underlying how S478 phosphorylation of TrkB regulates dendritic spine growth and remodeling, we examined BDNF-induced signaling pathways in cultured cortical neurons derived from *Trkb*$^{S478A/S478A}$ mice. BDNF-induced tyrosine phosphorylation of TrkB was normal in *Trkb*$^{S478A/S478A}$ neurons (**Fig. 3a**), which is consistent with our previous finding that Cdk5 does not regulate TrkB tyrosine phosphorylation[17]. Moreover, the induction of phospho-ERK and phosho-AKT by BDNF, which depends on TrkB phosphorylation at Y515 (ref. 16), was also unaffected in *Trkb*$^{S478A/S478A}$ neurons. Next, we explored the potential role of TrkB S478 phosphorylation in regulating Rho GTPases. We focused on the Rho GTPase Rac1, a well-established signaling protein that promotes spine growth and maturation by regulating actin dynamics[22,23]. Among the different Rac GEFs, TIAM1 has been reported to interact with TrkB[24]. Consistent with this, we found that TIAM1 was recruited to TrkB and became phosphorylated at Y829 after BDNF treatment (**Fig. 3b**). We found that TIAM1 was colocalized with phospho-S478 TrkB in cultured hippocampal neurons (**Supplementary Fig. 6a**), raising the possibility that S478 phosphorylation of TrkB might regulate BDNF-triggered TIAM1 activation. To test this possibility, we investigated whether the interaction between TIAM1 and TrkB was affected by S478 phosphorylation. Overexpression in 293T cells revealed that the amount of TrkB S478A mutant that was co-immunoprecipitated with TIAM1 was substantially reduced compared with wild-type TrkB (**Fig. 3c**). In contrast, the interaction between TrkB and TIAM1 did not require Y829 phosphorylation of TIAM1 (**Supplementary Fig. 6b**). Overexpressed wild-type TrkB also induced stronger Y829 phosphorylation of TIAM1 in 293T cells as compared to the S478A TrkB mutant (**Supplementary Fig. 6c**). Notably, TIAM1 was co-immunoprecipitated with TrkB only in the brain lysate of *Trkb*$^{WT/WT}$ control mice (**Fig. 3d**), indicating that S478 phosphorylation of TrkB is required for its interaction with TIAM1 *in vivo*. In addition, treatment with BDNF induced Y829 phosphorylation of TIAM1 in *Trkb*$^{WT/WT}$ cortical neurons but not the *Trkb*$^{S478A/S478A}$ neurons (**Fig. 3e**). These observations strongly suggest that S478 phosphorylation of TrkB is essential for its signaling to TIAM1.

To determine whether TIAM1 is essential for BDNF-induced spine morphogenesis, we expressed dominant-negative pleckstrin homology, coiled-coil and extra (PHCCEx) domain of TIAM1 along with GFP in cultured hippocampal neurons. The spine density and area was then examined with or without BDNF treatment. Expression of dominant-negative TIAM1 significantly reduced ($P < 0.05$) the density and area of dendritic spines without BDNF treatment. Notably, the induction of spine formation and enlargement by BDNF was completely abolished in neurons expressing dominant-negative TIAM1 (**Fig. 3f**). Taken together, our findings suggest that S478 phosphorylation of TrkB is crucial for its interaction with TIAM1 and the subsequent tyrosine phosphorylation during BDNF-induced spine morphogenesis.

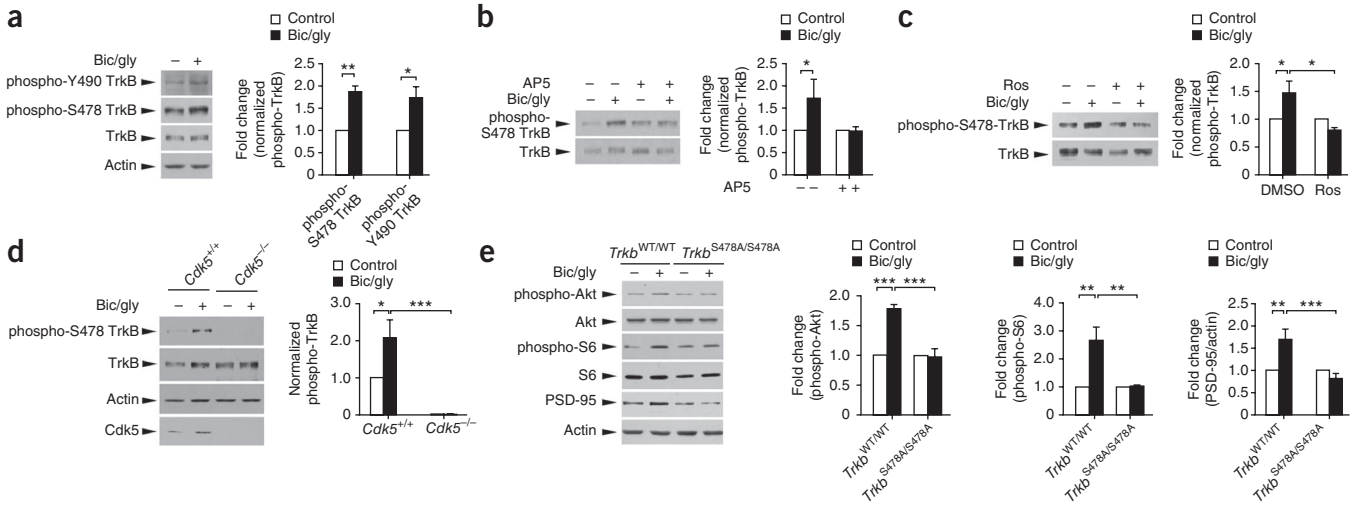

Figure 5 Cdk5-mediated phosphorylation of TrkB at S478 is required for increased S6 phosphorylation and PSD-95 expression following NMDA receptor activation. (**a**) Treatment of cultured cortical neurons (14 DIV) with bicuculline (20 μM) and glycine (200 μM, 15 or 30 min) increased TrkB phosphorylation at both Y490 and S478 (pooled from three experiments; $*P < 0.05$, $**P < 0.01$, Student's *t*-test). (**b**) The induction of TrkB phosphorylation at S478 was abolished in the presence of the NMDA receptor antagonist AP5 (200 μM, 30min; pooled from four experiments, $*P < 0.05$, one-way ANOVA, Bonferroni's multiple comparison test). (**c**) The Cdk5 inhibitor roscovitine (Ros, 10 μM) abolished the NMDA receptor–induced TrkB phosphorylation at S478 (pooled from three experiments, $*P < 0.05$, one-way ANOVA, Newman-Keuls multiple comparison test). (**d**) The induced TrkB phosphorylation was absent in cortical neurons derived from *Cdk5*$^{-/-}$ mice (pooled from four experiments, and neurons were cultured from four mice for each genotype, $*P < 0.05$, $***P < 0.001$, one-way ANOVA, Tukey's multiple comparison test). (**e**) Treatment of control (*Trkb*$^{WT/WT}$) cortical neurons with bicuculline and glycine (15 min for phospho-Akt; 30 min for phospho-S6 and PSD-95) significantly increased phosphorylation of Akt and S6 ribosomal protein, and expression of PSD-95. The induction was absent in *Trkb*$^{S478A/S478A}$ mutant neurons (for phospho-Akt and phospho-S6, data were pooled from three experiments and neurons were cultured from three mice for each genotype; for PSD-95, data were pooled from five experiments with neurons being cultured from five mice for each genotype; $**P < 0.01$, $***P < 0.001$, one way ANOVA, Tukey multiple comparison test). Full-length blots were presented in **Supplementary Figure 11**. Data were expressed as mean ± s.e.m.

S478 phosphorylation is required for TIAM1 signaling

We then asked whether TrkB phosphorylation at S478 is required for BDNF-induced activity of the Rho GTPases Rac1 and Cdc42. We performed pulldown assays using the p21-binding domain of Pak (Pak-PBD), which indicated the amount of GTP-bound (active) Rac1. Treatment of cultured cortical neurons with BDNF increased Rac1 activity in a Cdk5-dependent manner, as the induction was abolished by roscovitine and in *Cdk5*$^{-/-}$ neurons (**Fig. 4a**,**b**). Moreover, BDNF-induced Rac1 activation depended on TIAM1, as the induction was blocked by the expression of dominant-negative TIAM1 (**Fig. 4c**). Consistent with our hypothesis that S478 phosphorylation of TrkB regulates TIAM1 function, we found that BDNF failed to activate Rac1 in neurons from *Trkb*$^{S478A/S478A}$ mice (**Fig. 4d**). In contrast, BDNF-induced Cdc42 activity was not affected in *Trkb*$^{S478A/S478A}$ neurons (**Supplementary Fig. 7**). This suggests that the defect in BDNF-induced spine morphogenesis is a result of impaired activation of Rac1 rather than Cdc42.

Activation of NMDA receptor increases Rac1 activity and the subsequent phosphorylation of PAK to promote spine growth[25–27]. Given the observed deficits in activity-dependent spine remodeling in *Trkb*$^{S478A/S478A}$ mutant neurons (**Fig. 2**), we reasoned that BDNF-TrkB signaling might mediate activity-induced Rac1 activation and phosphorylation of PAK, and that this induction could be impaired by the loss of TrkB S478 phosphorylation. We first examined whether TrkB is involved in NMDA receptor–dependent phosphorylation of PAK. A brief stimulation of cortical neurons with glutamate increased PAK phosphorylation, and this induction was significantly attenuated ($P < 0.05$) in the presence of TrkB-IgG (a recombinant fusion protein comprising the extracellular domain of human TrkB and IgG), which scavenges endogenous BDNF (**Fig. 4e**). Notably, the induction of PAK phosphorylation by glutamate was significantly reduced ($P < 0.05$) in *Trkb*$^{S478A/S478A}$ cortical neurons (**Fig. 4f**). These findings suggest that S478 phosphorylation of TrkB is required for the activation of the Rac-PAK pathway by the NMDA receptor.

In addition to reorganization of actin cytoskeleton through Rac1 and PAK, activity-dependent spine remodeling also requires protein synthesis[8]. BDNF and the mTOR signaling pathway have been implicated in protein synthesis during L-LTP[28]. In addition to its anticipated function in regulating Rac1 activity, TIAM1 can also directly regulate the PI3K-AKT and mTOR pathway[25,29]. We therefore asked whether serine phosphorylation of TrkB might also regulate NMDA receptor–dependent protein synthesis. To this end, we treated cultured cortical neurons with bicuculline and the NMDA receptor co-factor glycine to activate synaptic NMDA receptors[30]. We found that treatment with bicuculline and glycine increased both tyrosine (Y490) and S478 phosphorylation of TrkB (**Fig. 5a**). The increase in S478 phosphorylation was mediated by NMDA receptor and required Cdk5, as it was blocked by the NMDA receptor antagonist D(−)-2-amino-5-phosphonovaleric acid (AP5) and the Cdk5 inhibitor roscovitine, as well as in *Cdk5*$^{-/-}$ neurons (**Fig. 5b–d**).

Next, we examined the phosphorylation of S6 ribosomal protein, a downstream target of mTOR and S6 kinase[31]. Treatment with bicuculline and glycine induced S6 phosphorylation in cultured cortical neurons. The induction was inhibited by AP5, TrkB-IgG and roscovitine, and was absent in *Cdk5*$^{-/-}$ neurons (**Supplementary Fig. 8a–c**). These observations indicate that NMDA receptor activation induces S6 phosphorylation in a BDNF- and Cdk5-dependent manner. Notably, the induced S6 phosphorylation after stimulation with bicuculline and glycine was greatly attenuated in *Trkb*$^{S478A/S478A}$ neurons (**Fig. 5e**), indicating a crucial role for TrkB S478 phosphorylation.

The induction of Akt phosphorylation after stimulation with bicuculline and glycine was also reduced in *Trkb*$^{S478A/S478A}$ neurons. To further study the role of Cdk5-mediated TrkB phosphorylation in activity-dependent protein synthesis, we examined the expression of PSD-95, which is critically involved in structural and functional plasticity, and the translation of *Psd-95* (also known as *Dlg4*) mRNA is regulated during synaptic plasticity[32]. Stimulation with bicuculline and glycine increased the expression of PSD-95 in an NMDA receptor– and mTOR-dependent manner (**Supplementary Fig. 8**), and the increase was abolished in *Cdk5*$^{-/-}$, as well as *Trkb*$^{S478A/S478A}$, neurons (**Fig. 5e** and **Supplementary Fig. 8c**). Taken together, our findings suggest that TrkB S478 phosphorylation is required for NMDA receptor–dependent signaling pathways that regulate actin dynamics and protein synthesis for promoting spine remodeling.

Trkb$^{S478A/S478A}$ mice show impaired LTP and memory

The impairment of activity-dependent spine remodeling and relevant signal transduction in *Trkb*$^{S478A/S478A}$ neurons prompted us to investigate whether hippocampal LTP is also affected. To elucidate the role of p35 and TrkB S478 phosphorylation, we first examined the effect of exogenous BDNF on the potentiation of synaptic strength in neonatal slices[33]. BDNF application facilitated LTP in wild-type and *Trkb*$^{WT/WT}$ control mice, as indicated by the increase in field excitatory postsynaptic potential (fEPSP) amplitude. Notably, the effect of BDNF was completely abolished in hippocampal slices from either *p35*$^{-/-}$ (also known as *Cdk5r1*) or *Trkb*$^{S478A/S478A}$ mice (**Fig. 6a**). BDNF treatment also increased the fEPSP slope (as a percentage of baseline) in *p35*$^{+/+}$ and *Trkb*$^{WT/WT}$ mice (*p35*$^{+/+}$: before BDNF, 112.9 ± 2.8%; after BDNF, 148.6 ± 5.5%; *Trkb*$^{WT/WT}$: before BDNF, 118.6 ± 4.4%; after BDNF, 151.6 ± 4.9%; $P < 0.001$), and the increase was absent in *p35*$^{-/-}$ or *Trkb*$^{S478A/S478A}$ mice (*p35*$^{-/-}$: before BDNF, 112.7 ± 4.2%; after BDNF, 110.2 ± 4.2%; *Trkb*$^{S478A/S478A}$: before BDNF, 121.2 ± 2.9%; after BDNF, 117.9 ± 4.9%; $P > 0.05$). We then investigated whether TrkB S478 phosphorylation is required for LTP in adult hippocampal slices that depend on endogenous BDNF. It was previously shown that mice lacking p35 have normal hippocampal LTP induced by 100-Hz tetanus[34], a form of LTP that is independent of endogenous BDNF[35]. We therefore used theta-burst stimulation (TBS), which induces L-LTP that requires endogenous BDNF[36], to induce LTP in the CA3-CA1 synapses of hippocampal slices derived from *Trkb*$^{S478A/S478A}$ mice and wild-type littermates. Although LTP could be induced in both wild-type and *Trkb*$^{S478A/S478A}$ slices, the magnitude of the increase in fEPSP amplitude (as a percentage of baseline) 170–180 min after TBS was significantly less in *Trkb*$^{S478A/S478A}$ slices as compared to wild-type slices (wild type, 162.7 ± 6.6%; *Trkb*$^{S478A/S478A}$, 132.1 ± 6.0%; $P < 0.01$, Student's *t*-test; **Fig. 6b**). The fEPSP slope was also significantly reduced in *Trkb*$^{S478A/S478A}$ slices (wild type, 195.9 ± 7.7%; *Trkb*$^{S478A/S478A}$, 165.7 ± 8.0%; $P < 0.05$, Student's *t*-test). We also examined paired-pulse facilitation (PPF), which is a measure of the enhanced synaptic response by a second stimulus in short time intervals and represents a presynaptic form of short-term plasticity. Consistent with previous findings of normal PPF in TrkB conditional knockout hippocampus[16], we did not observe a significant difference ($P > 0.05$) in PPF between wild-type and *Trkb*$^{S478A/S478A}$ hippocampal slices (**Supplementary Fig. 9**). These findings indicate that the TrkB S478 phosphorylation–deficient mice have reduced LTP at CA3-CA1 synapses but retain normal presynaptic function.

Finally, we examined whether the *Trkb*$^{S478A/S478A}$ mice exhibit impaired hippocampus-dependent learning and memory. *Trkb*$^{S478A/S478A}$ mutant mice and their wild-type littermates

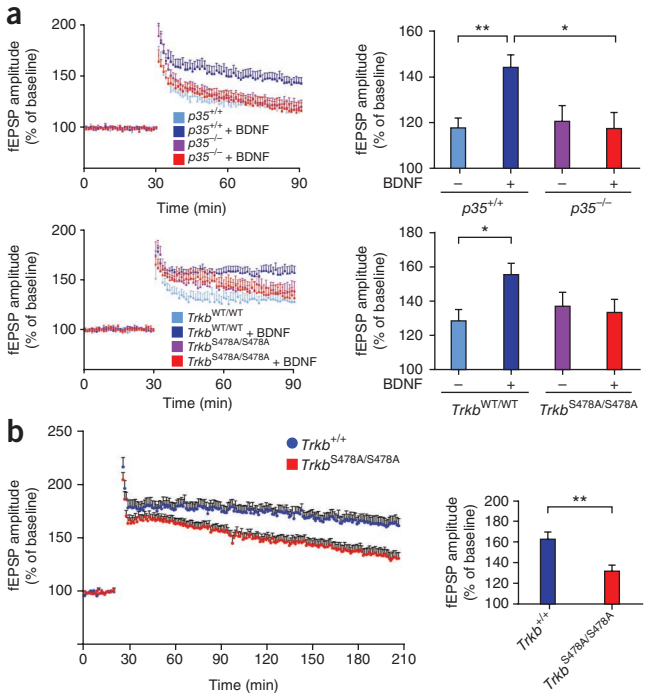

Figure 6 Impaired hippocampal LTP in *Trkb*$^{S478A/S478A}$ mutant mice. (**a**) BDNF-facilitated LTP in hippocampal slices was abolished in *p35*$^{-/-}$ mice (top) and *Trkb*$^{S478A/S478A}$ mice (bottom). Early phase LTP (E-LTP) was induced by a train of 100 Hz in the presence or absence of recombinant BDNF, and the fEPSP amplitude was recorded for 1 h after the tetanus. Exogenous BDNF significantly increased the fEPSP amplitude in wild-type *p35*$^{+/+}$ (control, $n = 15$ slices, 11 mice; BDNF, $n = 9$ slices, 3 mice; $^{**}P < 0.01$, one-way ANOVA; top) or the *Trkb*$^{WT/WT}$ control mice (control, $n = 10$ slices, 6 mice; BDNF, $n = 9$ slices, 5 mice; $^{*}P < 0.05$, one-way ANOVA; bottom). The facilitation effect of BDNF was abolished in both the *p35*$^{-/-}$ mice (control, $n = 10$ slices, 4 mice; BDNF, $n = 9$ slices, 3 mice; top) and *Trkb*$^{S478A/S478A}$ mutant mice (control, $n = 7$ slices, 5 mice; BDNF, $n = 6$ slices, 4 mice; bottom). (**b**) TBS-induced LTP at the CA3-CA1 synapses of hippocampal slices from wild-type (*Trkb*$^{+/+}$) ($n = 16$ slices, 7 mice) or *Trkb*$^{S478A/S478A}$ mutant ($n = 17$ slices, 8 mice). Quantification indicated that the fold change in average fEPSP amplitude 170–180 min after TBS stimulation was significantly reduced in the *Trkb*$^{S478A/S478A}$ mice when compared with wild-type mice ($^{**}P < 0.01$, Student's *t*-test). Data were expressed as mean ± s.e.m.

(4–5 months old) were subjected to the Morris water maze behavioral test, in which mice were trained to swim in a water tank of opaque water in the presence of external visual cues, and the time to reach the hidden platform (escape latency) was determined on each training day. After the last training day, a probe trial was performed in which the platform was removed, and the percentage of time which the mice spent in the targeted quadrant was measured. In the probe trial, wild-type mice (*Trkb*$^{+/+}$) spent significantly more time in the targeted quadrant than the other quadrants ($P < 0.001$, one-way ANOVA), indicating that they were able to locate the position of the hidden platform on the basis of spatial memory of the visual cues (**Fig. 7a**). In contrast, the *Trkb*$^{S478A/S478A}$ mice did not show any quadrant preference in the probe trial, as the time spent in the targeted quadrant was not significantly different from the time spent in the other quadrants ($P > 0.05$, one-way ANOVA) and was close to that of chance (25%). The time that the *Trkb*$^{S478A/S478A}$ mice spent in the targeted quadrant was also significantly reduced when compared with wild-type littermates ($P < 0.05$, two-way

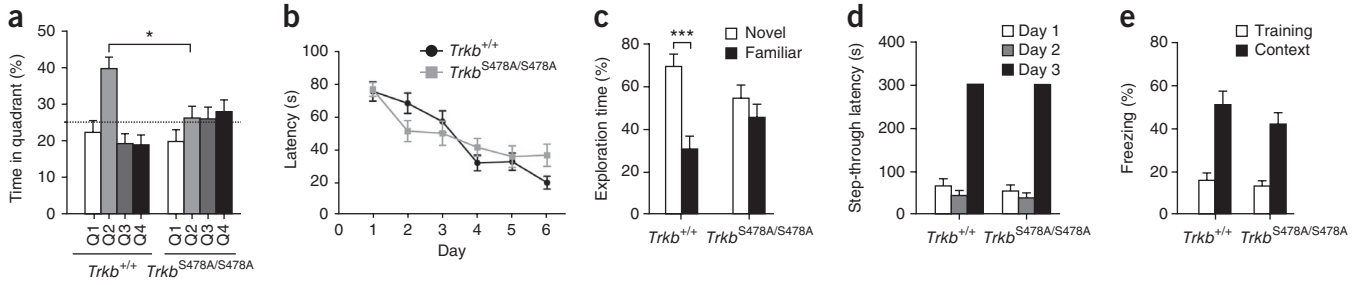

Figure 7 *Trkb*$^{S478A/S478A}$ mice display impaired memory in Morris water maze and novel object recognition, but have normal fear memory. (**a**) Wild-type (*Trkb*$^{+/+}$, $n = 16$) and *Trkb*$^{S478A/S478A}$ ($n = 15$) littermates were tested in a Morris water maze. *Trkb*$^{+/+}$ mice spent significantly more time in the target quadrant (Q2) than any of the other quadrants in the probe trial ($P < 0.001$, one-way ANOVA, Newman-Keuls multiple comparison test). For *Trkb*$^{S478A/S478A}$ mice, the time spent in the target quadrant was similar to that spent in the other quadrants ($P > 0.05$, one-way ANOVA, Newman-Keuls multiple comparison test). Compared with wild-type mice, the target quadrant occupancy of *Trkb*$^{S478A/S478A}$ mice was also significantly reduced ($^*P < 0.05$, two-way ANOVA, Bonferroni multiple comparison test). The dotted line indicates the chance level (25%). Swimming velocity was similar between *Trkb*$^{+/+}$ and *Trkb*$^{S478A/S478A}$ mice (*Trkb*$^{+/+}$ = 21.73 ± 0.57 cm s^{-1}, *Trkb*$^{S478A/S478A}$ = 21.76 ± 0.64 cm s^{-1}; $P > 0.05$, Student's *t*-test). (**b**) Escape latency between *Trkb*$^{+/+}$ and *Trkb*$^{S478A/S478A}$ mice in the Morris water maze was similar on any given training day ($P > 0.05$, two-way ANOVA, Bonferroni multiple comparison test). (**c**) In the novel object recognition task, *Trkb*$^{+/+}$ mice ($n = 11$), but not *Trkb*$^{S478A/S478A}$ mice ($n = 10$), preferred to explore the novel object during test day (three experiments, $^{***}P < 0.001$; one-way ANOVA, Tukey multiple comparison test). (**d**) In the passive avoidance task, the step through latency on day 3 (24 h after foot-shock) was similar between *Trkb*$^{+/+}$ ($n = 6$) and *Trkb*$^{S478A/S478A}$ mice ($n = 5$) ($P > 0.05$, one-way ANOVA, Newman-Keuls multiple comparison test). (**e**) There was no significant difference in percent freezing between *Trkb*$^{+/+}$ ($n = 8$) and *Trkb*$^{S478A/S478A}$ mice ($n = 13$) in contextual fear conditioning ($P > 0.05$, one-way ANOVA, Tukey multiple comparison test). Data are expressed as mean ± s.e.m. in all panels.

ANOVA; **Fig. 7a**), further highlighting the spatial memory deficit of the mutant mice. On the other hand, there was no significant difference in escape latency between the wild-type and *Trkb*$^{S478A/S478A}$ mice during training ($P > 0.05$, two-way ANOVA; **Fig. 7b**), suggesting that both the wild-type and mutant mice could similarly acquire spatial learning, and the mutant mice had visual acuity, motor coordination and swimming ability comparable to that of wild-type animals. The defective performance in the probe trial, which is a more sensitive measure of reference memory than escape latency[37–39], strongly suggests that the *Trkb*$^{S478A/S478A}$ mutant mice have impaired spatial memory. To rule out the possibility that the spatial memory deficit displayed by the *Trkb*$^{S478A/S478A}$ mice was a result of the insertion of the *loxP* site during genetic manipulation, we also examined the spatial learning and memory for the *Trkb*$^{WT/WT}$ control mouse line. Unlike the *Trkb*$^{S478A/S478A}$ mice, the *Trkb*$^{WT/WT}$ mice showed quadrant preference and performed similarly in the probe trial to their wild-type littermates (**Supplementary Fig. 10**). Thus, we conclude that the observed spatial memory deficits of the *Trkb*$^{S478A/S478A}$ mice were a result of the lack of TrkB S478 phosphorylation.

In addition to the Morris water maze, the wild-type and *Trkb*$^{S478A/S478A}$ mice were subjected to a novel object recognition task, which is also hippocampus-dependent and requires BDNF[40,41]. On the day of habituation, the distance traveled by the *Trkb*$^{S478A/S478A}$ mice was similar to that of the wild-type mice in the open field (wild type, 1,951 ± 108 cm; *Trkb*$^{S478A/S478A}$, 2,158 ± 109 cm; $P > 0.05$, Student's *t*-test). On the test day, wild-type mice spent significantly more time exploring the novel object ($P < 0.001$, one-way ANOVA), indicating that the mice could remember the familiar object and distinguish it from the novel one. In contrast, the *Trkb*$^{S478A/S478A}$ mice spent similar time exploring the novel and familiar objects ($P > 0.05$, one-way ANOVA), indicating impaired recognition (**Fig. 7c**). The impaired performance of the *Trkb*$^{S478A/S478A}$ knock-in mice in two different memory tasks suggests that TrkB S478 phosphorylation is essential for hippocampus-dependent memory formation. Notably, however, the *Trkb*$^{S478A/S478A}$ knock-in mice showed normal performance in contextual fear conditioning and passive avoidance (**Fig. 7d**,**e**). This is consistent with some earlier studies, which reported normal contextual fear conditioning and passive avoidance in BDNF and TrkB conditional knockout mice[16,40]. We therefore conclude that TrkB S478 phosphorylation is essential for memory formation in specific hippocampus-dependent learning tasks.

DISCUSSION

Elucidating the signaling pathways involved in NMDA receptor–dependent structural and functional modification of synapses is fundamental to our understanding of memory formation. One well-accepted notion is that protein phosphorylation is important for regulating the function of diverse synaptic proteins during synaptic plasticity. The BDNF receptor TrkB has been identified as one of the critical kinases that modulate activity-dependent changes in synaptic strength crucial for learning and memory[3]. Our results provide compelling evidence that serine phosphorylation of TrkB at S478 by Cdk5 is required for synaptic plasticity and memory formation. Mutant mice lacking the Cdk5-mediated phosphorylation of TrkB exhibited reduced LTP in the hippocampal CA3-CA1 synapses. This is associated with impaired performance in Morris water maze and novel object recognition. Mechanistically, we found that phospho-S478 TrkB was present at neuronal synapses and was required for functional interaction with the postsynaptic Rac GEF TIAM1. Notably, we observed attenuation of activity-dependent spine remodeling and NMDA receptor–dependent signal transduction in primary neurons that lacked TrkB S478 phosphorylation, which is consistent with TIAM1 being involved in activity-dependent spine morphogenesis[25]. To the best of our knowledge, our results represent the first genetic evidence that serine phosphorylation of an RTK has an important physiological function in neurons, and thus opens a new avenue in the study of neuronal signaling cross-talk between RTKs and serine/threonine kinases in regulating neuronal function.

Several serine/threonine kinases, including CaMKII, PKC, PKA and MAPK, have been reported to have specific roles in LTP and hippocampus-dependent learning. Recent findings have shown that Cdk5 is also a crucial regulator of synaptic plasticity and learning. Cdk5 activity is regulated following NMDA receptor activation[42], and studies using various Cdk5 and p35/p25 knockout and transgenic

mice have revealed altered synaptic plasticity and learning[18]. However, the precise role of Cdk5 in activity-dependent synaptic plasticity and memory formation remains enigmatic. For example, Cdk5 conditional knockout mice and p25 transgenic mice with transient increase in Cdk5 activity both exhibit enhanced synaptic plasticity and improved learning[43,44]. It is noteworthy that many different synaptic proteins, including ion channels, scaffold proteins, adhesion molecules and signaling proteins, have been identified as Cdk5 substrates, and the interaction and phosphorylation of different proteins with Cdk5 might lead to changes in synaptic strength in opposing directions[18]. For example, although phosphorylation of NR2A by Cdk5 increases conductance of the ion channel[45], Cdk5 also promotes calpain-mediated degradation of NR2B and negatively regulates the clustering of PSD-95 (refs. 44,46). In Cdk5 conditional knockout mice with enhanced memory, Cdk5 expression is reduced by ~50% rather than totally eliminated[44]. It is therefore possible that S478 phosphorylation of TrkB might not be largely affected in those mice and its involvement in synaptic plasticity and memory is masked by dysregulation of other Cdk5 substrates. This highlights the difficulty in deciphering how Cdk5 functions precisely in synaptic plasticity and learning by simply genetically manipulating the levels of Cdk5 and p35 expression. To gain further insights into Cdk5 function at the synapses, it is crucial to identify the Cdk5 phosphorylation sites of the synaptic proteins of interest and generate phosphorylation-deficient mutant. Consistent with this effort, we generated *Trkb*$^{S478A/S478A}$ mice on the basis of our previous findings that S478 of TrkB is the major Cdk5 phosphorylation site[17]. Our study is therefore distinguished from previous reports using Cdk5 and p35 transgenic mice by our attempt to specifically address the importance of Cdk5 in synaptic plasticity and memory formation with regard to its phosphorylation of one specific substrate.

The *Trkb*$^{S478A/S478A}$ hippocampal neurons showed reduced LTP mainly in the maintenance, rather than the induction, of LTP. What are the potential mechanisms that underlie impaired LTP maintenance in TrkB S478 phosphorylation–deficient neurons? One possibility involves deficits in spine remodeling. We found that the BDNF-induced spine growth and glutamate-induced spine enlargement were substantially attenuated in *Trkb*$^{S478A/S478A}$ hippocampal neurons, which is consistent with defects in signaling through the Rac GEF TIAM1. Given that BDNF-dependent spine remodeling has been implicated in the consolidation of synaptic plasticity[8,14,47], we favor the idea that the defect in spine morphogenesis contributes, at least in part, to the impaired LTP maintenance of the *Trkb*$^{S478A/S478A}$ hippocampal neurons. Nonetheless, it has been suggested that BDNF regulates different synaptic functions in both the pre- and post-synaptic sites[3]. It remains possible that TrkB S478 phosphorylation might also regulate synaptic function in addition to structural plasticity. *Trkb*$^{S478A/S478A}$ neurons showed normal PPF, suggesting that this pre-synaptic form of short-term plasticity does not depend on TrkB S478 phosphorylation. On the other hand, BDNF has been shown to promote AMPA receptor–mediated mEPSC in hippocampal neurons[48]. It would be interesting to know whether the expression and trafficking of AMPA receptors also depend on TrkB S478 phosphorylation.

Although tyrosine phosphorylation of an RTK is indispensible for signal propagation, much less is known about how serine phosphorylation affects the function of an RTK. The better characterized examples from early studies include EGF receptor and insulin receptor, whose kinase activities are negatively regulated following serine phosphorylation that might be involved in ligand-induced desensitization[49]. Previously, we found that kinase activity of ErbB can be modulated by serine phosphorylation[50]. In contrast with these studies, S478 phosphorylation did not seem to affect the kinase activity of TrkB, as BDNF-induced autophosphorylation at Y490 was normal in *Trkb*$^{S478A/S478A}$ neurons. How might the function of TrkB be regulated by serine phosphorylation? The surface and synaptic localization of TrkB was normal in *Trkb*$^{S478A/S478A}$ neurons. Although TrkB level was reduced (~20%) in the knock-in mice, we do not think this is the major reason to account for the defects of *Trkb*$^{S478A/S478A}$ mice/neurons, as we did not observe a corresponding reduction of BDNF-induced signaling (such as TrkB tyrosine phosphorylation and Cdc42 induction) in *Trkb*$^{S478A/S478A}$ neurons. Moreover, the effect of S478 phospho-deficient TrkB on spine growth was confirmed by exogenous expression of the TrkB S478A construct. Finally, it was previously reported that spatial memory in the Morris water maze was not affected in heterozygous TrkB mice, which showed an approximately twofold reduction in TrkB expression[15]. It is therefore unlikely that the small reduction in the level of TrkB expression in the *Trkb*$^{S478A/S478A}$ mice could explain their impaired memory in the Morris water maze. We propose that S478 phosphorylation does not grossly affect the expression, localization and general signaling capability of TrkB but instead regulates specific aspects of TrkB signaling, such as activation of the Rac GEF TIAM1.

Our results suggest that TIAM1 is crucial for mediating the activation of Rac1 by BDNF during spine morphogenesis, and failure to couple to TIAM1 activation in *Trkb*$^{S478A/S478A}$ neurons might account for the observed impairments in activity-dependent spine remodeling and signal transduction. The interaction between TIAM1 and TrkB, as well as TIAM1 Y829 phosphorylation, was completely absent in *Trkb*$^{S478A/S478A}$ mice. This suggests that S478 phosphorylation either enhances TrkB binding to TIAM1 directly or promotes recruitment of TIAM1 via interaction with other adaptor proteins. Given that TIAM1 is required for NMDA receptor–dependent spine growth, the lack of TIAM1 interaction with TrkB and its subsequent Y829 phosphorylation could explain the impaired activity-dependent spine enlargement observed in *Trkb*$^{S478A/S478A}$ neurons. Nonetheless, it is noteworthy that TIAM1 also acts downstream of receptors other than TrkB, including EphB receptor. This would explain why expression of dominant-negative TIAM1 resulted in more severe phenotypes in spine density than expression of the TrkB S478A mutant. In addition, the synaptic localization of TIAM1 was not affected in the *Trkb*$^{S478A/S478A}$ knock-in mice (data not shown), indicating that TIAM1 can interact with synaptic transmembrane proteins other than TrkB. Finally, TIAM1 has been shown to be unusual among different Rac GEFs because of its ability to regulate the activity of S6 kinase through Rac1[25,29]. Our finding that NMDA receptor–dependent phosphorylation of AKT and S6 ribosomal protein was impaired in *Trkb*$^{S478A/S478A}$ neurons might therefore be explained by the lack of functional interaction between TrkB and TIAM1. Whether TIAM1-deficient mice exhibit deficits in protein synthesis–dependent long-term synaptic plasticity and spatial memory remains to be investigated.

METHODS

Methods and any associated references are available in the online version of the paper.

Note: Supplementary information is available in the online version of the paper.

ACKNOWLEDGMENTS

We are grateful to A. Kulkarni (National Institutes of Health) and T. Curran (University of Pennsylvania) for the *Cdk5*$^{-/-}$ mice, L.-H. Tsai (Massachusetts Institute of Technology) for the *p35*$^{-/-}$ mice, M. Greenberg (Harvard Medical School) for the phospho-TIAM1 and phospho-PAK antibodies, W. Mobley (University of California, San Diego) for TIAM1 expression constructs, and

L. Reichardt (University of California, San Francisco) for the chicken antibody to TrkB. We thank C. Kwong, B. Lai, P. Sun, B. Butt, Y. Liang, H. Chuang, Y. Dai and K. Ho for their excellent technical assistance, Amy Fu and Ada Fu for critical reading of the manuscript, and members of the Ip laboratory for many helpful discussions. This study was supported in part by the Research Grants Council of Hong Kong (HKUST 661109, 661309, 660810, 661010 and 661111), the Area of Excellence Scheme of the University Grants Committee (AoE/B-15/01) and the S.H. Ho Foundation. N.Y.I. was the recipient of Croucher Foundation Senior Research Fellowship, and K.-O.L. and Z.H.C. were the recipients of Croucher Foundation Research Fellowship. M.E.P. and L.T. were supported by the Intramural Research Program of the National Cancer Institute, Center for Cancer Research, US National Institutes of Health.

AUTHOR CONTRIBUTIONS

K.-O.L. and N.Y.I. supervised the project. K.-O.L., A.S.L.W., Z.H.C. and N.Y.I. designed the experiments. K.-O.L., A.S.L.W., M.-C.C., P.X., Z.L. and K.-C.L. conducted the experiments. K.-O.L., A.S.L.W., M.-C.C., P.X., Z.L., K.-C.L. and N.Y.I. carried out the data analyses. W.-H.Y. designed and carried out the data analyses of the electrophysiology experiments and H.X. performed the electrophysiology experiments and data analysis. L.T. and M.E.P designed and generated the knock-in mice. K.-O.L., Z.H.C. and N.Y.I. wrote the manuscript.

COMPETING FINANCIAL INTERESTS

The authors declare no competing financial interests.

Published online at http://www.nature.com/doifinder/10.1038/nn.3237.
Reprints and permissions information is available online at http://www.nature.com/reprints/index.html.

1. Huang, E.J. & Reichardt, L.F. Trk receptors: roles in neuronal signal transduction. *Annu. Rev. Biochem.* **72**, 609–642 (2003).
2. Kandel, E.R. The molecular biology of memory storage: a dialogue between genes and synapses. *Science* **294**, 1030–1038 (2001).
3. Lu, Y., Christian, K. & Lu, B. BDNF: A key regulator for protein synthesis–dependent LTP and long-term memory? *Neurobiol. Learn. Mem.* **89**, 312–323 (2008).
4. Engert, F. & Bonhoeffer, T. Dendritic spine changes associated with hippocampal long-term synaptic plasticity. *Nature* **399**, 66–70 (1999).
5. Maletic-Savatic, M., Malinow, R. & Svoboda, K. Rapid dendritic morphogenesis in CA1 hippocampal dendrites induced by synaptic activity. *Science* **283**, 1923–1927 (1999).
6. Matsuzaki, M., Honkura, N. & Ellis-Davies, G.C.R. & Kasai, H. Structural basis of long-term potentiation in single dendritic spines. *Nature* **429**, 761–766 (2004).
7. Fukazawa, Y. *et al.* Hippocampal LTP is accompanied by enhanced F-actin content within the dendritic spine that is essential for late LTP maintenance *in vivo*. *Neuron* **38**, 447–460 (2003).
8. Tanaka, J. *et al.* Protein synthesis and neurotrophin-dependent structural plasticity of single dendritic spines. *Science* **319**, 1683–1687 (2008).
9. Chen, Z.Y. *et al.* Genetic variant BDNF (Val66Met) polymorphism alters anxiety-related behavior. *Science* **314**, 140–143 (2006).
10. An, J.J. *et al.* Distinct role of long 3' UTR BDNF mRNA in spine morphology and synaptic plasticity in hippocampal neurons. *Cell* **134**, 175–187 (2008).
11. Ninan, I. *et al.* The BDNF Val66Met polymorphism impairs NMDA receptor–dependent synaptic plasticity in the hippocampus. *J. Neurosci.* **30**, 8866–8870 (2010).
12. Tyler, W.J. & Pozzo-Miller, L.D. BDNF enhances quantal neurotransmitter release and increases the number of docked vesicles at the active zones of hippocampal excitatory synapses. *J. Neurosci.* **21**, 4249–4258 (2001).
13. Ji, Y., Pang, P.T., Feng, L. & Lu, B. Cyclic AMP controls BDNF-induced TrkB phosphorylation and dendritic spine formation in mature hippocampal neurons. *Nat. Neurosci.* **8**, 164–172 (2005).
14. Rex, C.S. *et al.* Brain-derived neurotrophic factor promotes long-term potentiation–related cytoskeletal changes in adult hippocampus. *J. Neurosci.* **27**, 3017–3029 (2007).
15. Minichiello, L. *et al.* Essential role for TrkB receptors in hippocampus-mediated learning. *Neuron* **24**, 401–414 (1999).
16. Minichiello, L. *et al.* Mechanism of TrkB-mediated hippocampal long-term potentiation. *Neuron* **36**, 121–137 (2002).
17. Cheung, Z.H., Chin, W.H., Chen, Y., Ng, Y.P. & Ip, N.Y. Cdk5 is involved in BDNF-stimulated dendritic growth in hippocampal neurons. *PLoS Biol.* **5**, e63 (2007).
18. Lai, K.O. & Ip, N.Y. Recent advances in understanding the roles of Cdk5 in synaptic plasticity. *Biochim. Biophys. Acta* **1792**, 741–745 (2009).
19. Matsuzaki, M. *et al.* Dendritic spine geometry is critical for AMPA receptor expression in hippocampal CA1 pyramidal neurons. *Nat. Neurosci.* **4**, 1086–1092 (2001).
20. Harvey, C.D. & Svoboda, K. Locally dynamic synaptic learning rules in pyramidal neuron dendrites. *Nature* **450**, 1195–1200 (2007).
21. Korkotian, E. & Segal, M. Morphological constraints on calcium-dependent glutamate receptor trafficking into individual dendritic spine. *Cell Calcium* **42**, 41–57 (2007).
22. Nakayama, A.Y. & Luo, L.Q. Intracellular signaling pathways that regulate dendritic spine morphogenesis. *Hippocampus* **10**, 582–586 (2000).
23. Tashiro, A., Minden, A. & Yuste, R. Regulation of dendritic spine morphology by the Rho family of small GTPases: antagonistic roles of Rac and Rho. *Cereb. Cortex* **10**, 927–938 (2000).
24. Miyamoto, Y., Yamauchi, J., Tanoue, A., Wu, C. & Mobley, W.C. TrkB binds and tyrosine-phosphorylates Tiam1, leading to activation of Rac1 and induction of changes in cellular morphology. *Proc. Natl. Acad. Sci. USA* **103**, 10444–10449 (2006).
25. Tolias, K.F. *et al.* The Rac1-GEF Tiam1 couples the NMDA receptor to the activity-dependent development of dendritic arbors and spines. *Neuron* **45**, 525–538 (2005).
26. Xie, Z. *et al.* Kalirin-7 controls activity-dependent structural and functional plasticity of dendritic spines. *Neuron* **56**, 640–656 (2007).
27. Saneyoshi, T. *et al.* Activity-dependent synaptogenesis: regulation by a CaM-kinase kinase/CaM-kinase I/beta PIX signaling complex. *Neuron* **57**, 94–107 (2008).
28. Barco, A. *et al.* Gene expression profiling of facilitated L-LTP in VP16-CREB mice reveals that BDNF is critical for the maintenance of LTP and its synaptic capture. *Neuron* **48**, 123–137 (2005).
29. Buchsbaum, R.J., Connolly, B.A. & Feig, L.A. Regulation of p70 S6 kinase by complex formation between the rac guanine nucleotide exchange factor (Rac-GEF) Tiam1 and the scaffold spinophilin. *J. Biol. Chem.* **278**, 18833–18841 (2003).
30. Lu, W. *et al.* Activation of synaptic NMDA receptors induces membrane insertion of new AMPA receptors and LTP in cultured hippocampal neurons. *Neuron* **29**, 243–254 (2001).
31. Richter, J.D. & Klann, E. Making synaptic plasticity and memory last: mechanisms of translational regulation. *Genes Dev.* **23**, 1–11 (2009).
32. Todd, P.K., Mack, K.J. & Malter, J.S. The fragile X mental retardation protein is required for type-I metabotropic glutamate receptor-dependent translation of PSD-95. *Proc. Natl. Acad. Sci. USA* **100**, 14374–14378 (2003).
33. Figurov, A., Pozzo-Miller, L.D., Olafsson, P., Wang, T. & Lu, B. Regulation of synaptic responses to high-frequency stimulation and LTP by neurotrophins in the hippocampus. *Nature* **381**, 706–709 (1996).
34. Ohshima, T. *et al.* Impairment of hippocampal long-term depression and defective spatial learning and memory in p35 mice. *J. Neurochem.* **94**, 917–925 (2005).
35. Kang, H., Welcher, A.A., Shelton, D. & Schuman, E.M. Neurotrophins and time: different roles for TrkB signaling in hippocampal long-term potentiation. *Neuron* **19**, 653–664 (1997).
36. Patterson, S.L. *et al.* Some forms of cAMP-mediated long-lasting potentiation are associated with release of BDNF and nuclear translocation of phospho-MAP kinase. *Neuron* **32**, 123–140 (2001).
37. Abel, T. *et al.* Genetic demonstration of a role for PKA in the late phase of LTP and in hippocampus-based long-term memory. *Cell* **88**, 615–626 (1997).
38. Miller, S. *et al.* Disruption of dendritic translation of CaMKIIalpha impairs stabilization of synaptic plasticity and memory consolidation. *Neuron* **36**, 507–519 (2002).
39. Kelleher, R.J. III, Govindarajan, A., Jung, H.Y., Kang, H. & Tonegawa, S. Translational control by MAPK signaling in long-term synaptic plasticity and memory. *Cell* **116**, 467–479 (2004).
40. Heldt, S.A., Stanek, L., Chhatwal, J.P. & Ressler, K.J. Hippocampus-specific deletion of BDNF in adult mice impairs spatial memory and extinction of aversive memories. *Mol. Psychiatry* **12**, 656–670 (2007).
41. Rampon, C. *et al.* Enrichment induces structural changes and recovery from nonspatial memory deficits in CA1 NMDAR1-knockout mice. *Nat. Neurosci.* **3**, 238–244 (2000).
42. Wei, F.Y. *et al.* Control of cyclin-dependent kinase 5 (Cdk5) activity by glutamatergic regulation of p35 stability. *J. Neurochem.* **93**, 502–512 (2005).
43. Fischer, A., Sananbenesi, F., Pang, P.T., Lu, B. & Tsai, L.H. Opposing roles of transient and prolonged expression of p25 in synaptic plasticity and hippocampus-dependent memory. *Neuron* **48**, 825–838 (2005).
44. Hawasli, A.H. *et al.* Cyclin-dependent kinase 5 governs learning and synaptic plasticity via control of NMDAR degradation. *Nat. Neurosci.* **10**, 880–886 (2007).
45. Li, B.S. *et al.* Regulation of NMDA receptors by cyclin-dependent kinase-5. *Proc. Natl. Acad. Sci. USA* **98**, 12742–12747 (2001).
46. Morabito, M.A., Sheng, M. & Tsai, L.H. Cyclin-dependent kinase 5 phosphorylates the N-terminal domain of the postsynaptic density protein PSD-95 in neurons. *J. Neurosci.* **24**, 865–876 (2004).
47. Bramham, C.R. Local protein synthesis, actin dynamics and LTP consolidation. *Curr. Opin. Neurobiol.* **18**, 524–531 (2008).
48. Bolton, M.M., Pittman, A.J. & Lo, D.C. Brain-derived neurotrophic factor differentially regulates excitatory and inhibitory synaptic transmission in hippocampal cultures. *J. Neurosci.* **20**, 3221–3232 (2000).
49. van der Geer, P., Hunter, T. & Lindberg, R.A. Receptor protein-tyrosine kinases and their signal transduction pathways. *Annu. Rev. Cell Biol.* **10**, 251–337 (1994).
50. Fu, A.K. *et al.* Cdk5 is involved in neuregulin-induced AChR expression at the neuromuscular junction. *Nat. Neurosci.* **4**, 374–381 (2001).

ONLINE METHODS

Generation of the *Trkb*$^{WT/WT}$ and *Trkb*$^{S478A/S478A}$ transgenic mice. For targeting the exon containing S478 in the *Trkb* locus, a targeting vector was constructed using a C57Bl/6J mouse bacterial artificial chromosome (BAC clone 10719 from the RPCI-23 BAC Resource library, Children's Hospital Oakland Research Institute)[51]. The nucleotides encoding codons serine 476, alanine 477 and serine 478 were mutated from 5′-TCTGCCAGC-3′ to 5′-TCTGCAGCA-3′ to incorporate a PstI site and to change Ser478 to alanine. After introducing this mutation in the BAC, a 9.6-kb DNA fragment spanning a 5-kb upstream and 4.4-kb downstream sequence of exon 12 was retrieved into pBluescript II containing a diphtheria toxin A chain cassette used for negative selection. A neomycin-resistance cassette flanked by *loxP* sites was inserted 450 bp downstream of exon 12. The targeting vectors were then linearized and used for gene targeting in the v6.4 embryonic stem (ES) cell line as described elsewhere[52]. DNAs derived from G418-resistant ES cell clones were screened by StuI and EcoRI digestion using a 5′ and 3′ probe external to the targeting vector sequence, respectively. PstI digestion using the internal probe (**Supplementary Fig. 1**) was used to screen for the S478 mutation. Recombinant clones were obtained at a frequency of 1 in 6. Two targeted ES cell clones for both the wild-type and S478A mutant alleles were injected into C57Bl/6 blastocysts to generate chimeras that transmitted the mutated allele to the progeny[53]. Mice with the targeted mutation were bred to a β-actin–cre transgenic mouse to remove the neomycin-resistance cassette. Mice were bred in a specific pathogen–free facility with food and water *ad libitum*. Animals were housed at 12-h light-dark cycle (lights were on 7:00 to 19:00) at 22 °C. All animal studies were approved by the Animal Care Committee at the Hong Kong University of Science and Technology in accordance with institutional guidelines.

DNA constructs, chemicals and antibodies. The Flag-tagged TIAM1-C1199 and TIAM1 PHCCEx constructs were gifts from W. Mobley (University of California, San Diego). TrkB expression constructs were described previously[17]. Bicuculline, glycine and L-glutamic acid were purchased from Sigma, DL-AP5 and MNI-glutamate from Tocris, and TrkB-IgG from R&D Systems. The rabbit polyclonal antibody to phospho-S478 TrkB (1:3,000) was raised from synthetic peptide (CISNDDDSApSPLHHIS) as previously described[17]. The antibodies to phospho-TIAM1 (Y829) (1:1,000) and phospho-PAK (1:2,000) were gifts from M. Greenberg (Harvard Medical School). The chicken antibody to the TrkB extracellular domain (1:200) was a gift from L. Reichardt (University of California, San Francisco). We also used antibodies to PSD-95 (1:1,000, Thermo Scientific MA1-046), TrkB (1:1,300, BD Biosciences 610102), actin (1:6,000, Sigma A3853), Cdk5 (1:500, DC17, Santa Cruz) and TIAM1 (1:500, C16, Santa Cruz) as primary antibodies. Antibodies to p35 (1:1,000, 2680), AKT (1:3,000, 9272), S6 ribosomal protein (1:2,000, 2317), PAK (1:1,000, 2602), ERK (1:1,000, 9102), phospho-TrkA (Y490) (1:500, 9141), phospho-AKT (S473) (1:2,000, 9271), phospho-S6 (S235/236) (1:1,000, 4856) and phospho-ERK (T202/Y204) (1:4,000, 9101) were from Cell Signaling, as were horseradish peroxidase–conjugated goat antibodies to rabbit (1:2,000–4,000, 7074) and mouse (1:2,000–8,000, 7076). Alexa Fluor 488–conjugated (A-11008 and A-11001) or Alexa Fluor 546–conjugated (A-11010 and A-11003) secondary antibodies (1:2,000) were from Molecular Probes.

Behavioral studies. In the Morris water maze, the hidden platform procedure was performed in a circular tank (diameter, 1.8 m) filled with opaque water. The swimming path of the mouse was recorded by video camera and analyzed by Ethovision XT version 7.0 (Noldus software). For training, the male mouse (4–5 months old) was placed in the tank at four random points. The mouse was allowed to search for the platform for 90 s. Two training trials were given every day and the latency for each trial was recorded. Probe trial was performed on day 6 or 7. The mouse was allowed to swim in the tank for 90 s without the platform, and performance was assessed on the basis of the time spent in the quadrant in which the hidden platform was originally located. In the open field test, the mouse was placed in the center of an open top chamber (50 × 50 × 40 cm) and was allowed to explore in the arena for 30 min. The locomotor activity of the animal was recorded by video camera. In novel object recognition, the mouse (~3 months old) was allowed to acclimate in the open field box on day 1 for 5 min. On day 2, the mouse was subject to a training session, with two identical objects placed in the box. The mouse was allowed to explore for 5 min, and the amount of time spent at each object was recorded. Exploration of the object was characterized when the head of the mouse was facing and within 1 inch of the object or any part of the body, except the tail, was touching the object. On day 3, the mouse was placed in the same box, which contained the original object in the training session (familiar) and the new object (novel). The amount of time the mouse spent with each object was recorded. In passive avoidance, the mouse was placed in the lighted compartment and allowed to explore for 30 s. Then the door was raised and the mouse was allowed to explore freely. The latency to enter the dark compartment with all four paws was recorded. On day 2, the latency to enter the dark compartment was similarly recorded. We delivered a foot shock (0.5 mA, 2-s duration) 3 s after the door was closed. The mouse was removed to its home cage 30 s after the foot shock. On test day (24 h after training), the mouse was returned to the lighted compartment. After 5 s, the guillotine door was lifted, and the latency to enter the dark compartment was recorded. For contextual conditioning, the mouse was acclimatized to the conditioning chamber for 3 min, after which it was presented with one pairing of tone (85 dB and 2,800 Hz for 30 s) and foot shock (0.4 mA, administered during the last 2 s of the tone). The mouse was removed from the chamber 60 s after the last foot shock presentation. On test day (24 h after training), the mouse was transferred to the conditioning chamber for 5 min without tone and shock, and freezing behavior was recorded. All of the behavioral experiments were performed and analyzed blinded.

Electrophysiological measurements. Mice were decapitated and the brains were immediately removed and immersed in ice-cold artificial cerebrospinal fluid (ACSF; 125 mM NaCl, 2.0 mM KCl, 1.2 mM $MgSO_4$, 2.5 mM $CaCl_2$, 1.2 mM KH_2PO_4, 11 mM glucose and 26 mM $NaHCO_3$), which was continuously bubbled with 95% O_2 and 5% CO_2. Parasagittal sections (300 m) were cut using a vibrating microtome (Integraslice 7550MM, Campden Instruments). Slices were pre-incubated in oxygenated ACSF at 34 ± 1 °C for at least 1 h. Afterward, a slice was transferred to a submersion-type recording chamber perfused constantly with ACSF at a rate of 1.0–1.3 ml min^{-1}. The temperature of the ACSF in the recording chamber was maintained at 34 ± 1 °C by a heat exchanger.

A planar multi-electrode recording setup (MED64 system, Alpha Med Sciences) was used to record the fEPSP as described[54]. Each slice was superfused by 100 ml of oxygenated ACSF, which was re-circulated at a flow rate of 1–1.5 ml min^{-1}. fEPSPs were recorded from the dendritic layer of CA1 neurons by choosing an electrode in the Schaffer collateral pathway as the stimulating electrode. First, an input-output relationship was generated by delivering 10–100-μA electrical stimuli, and the amplitude of the peak fEPSPs was measured. A stimulation intensity that evoked the fEPSP with a magnitude of 30–40% of the maximum response was chosen. After allowing a stable baseline of 30 min, an induction protocol that evoked either E-LTP or L-LTP was applied. E-LTP induction protocol consists of one train of 100-Hz stimulus that lasted for 1 s, and the field potential response for 1 h after the tetanus was recorded. For L-LTP induction, we applied five spaced trains (inter-train intervals of 5 min), each of six theta bursts (100 Hz, interburst interval of 300 ms). The field potential was monitored for 3 h after the conditioning stimuli. The magnitude of L-LTP was quantified as the percentage change in the average amplitude of the fEPSP taken from 170–180-min interval after L-LTP induction, compared with that of the baseline average. To test the effect of BDNF, recombinant BDNF was diluted in ACSF containing 200 μg ml^{-1} bovine albumin, and re-circulated in a volume of 20 ml. To characterize the paired-pulse ratio, twin stimuli that were separated by a variable time interval (25, 50, 75, 100 or 200 ms) were delivered to the CA3-CA1 pathway ten times each, and the average ratio of the amplitude of the second evoked fEPSPs over the first one was determined. All the electrophysiology experiments were performed and analyzed blinded.

Cell culture and transfection. 293T cells were transfected using Lipofectamine 2000 (Invitrogen). Primary cortical and hippocampal neurons were prepared from embryonic day 18–19 rat embryos as previously described[52]. Cortical neurons (6×10^6 cells per 100 mm dish or 2.5×10^6 cells per 60 mm dish) were plated on poly-L-lysine–coated (0.1 mg ml^{-1}) dishes and fed with Neurobasal medium supplemented with 2% B27 (by volume) and 10 mM L-glucose. Rat hippocampal neurons were seeded on 18-mm coverslips coated with poly-D-lysine (1 mg ml^{-1}) (0.5×10^5 cells per coverslip for immunocytochemistry, 1.5×10^5 cells per coverslip for transfection with GFP expression construct). To study BDNF-induced spine formation, we serum-starved hippocampal neurons (9 DIV) with DMEM medium (Invitrogen) for 1 h at 37 °C before

doi:10.1038/nn.3237

transfecting them with different plasmids plus EmGFP using calcium phosphate precipitation as previously described[55].

Immunoprecipitation and western blot. Synaptosome and PSD fraction were prepared as described[52]. For most of the biochemical studies, cortical neurons were lysed by RIPA plus various protease and phosphatase inhibitors. For co-immunoprecipitation, HEK293T cells and cultured cortical neurons were lysed in Buffer A (20 mM Tris, pH 7.6, 50 mM NaCl, 1 mM EDTA, 1 mM NaF, 0.5% Nonidet P-40 (by volume)) with protease and phosphatase inhibitors. Rat brains were homogenized in phosphate-buffered saline (PBS) plus protease and phosphatase inhibitors. After low-speed centrifugation, the supernatant was diluted by equal volume of 2× Buffer A. Co-immunoprecipitation of HEK293T cell or whole brain lysate was performed in Buffer A. Lysate (1 mg for HEK293T cells, 2 mg for cultured cortical neurons or brain homogenate) was incubated with the corresponding antibody (1–2 μg) at 4 °C for either 2 h or overnight and then incubated with 50 μl of protein G–Sepharose at 4 °C for 1 h. Samples were washed with buffer A and resuspended in SDS sample buffer. Co-immunoprecipitated proteins were detected by western blot. Densitometric quantification of protein band intensity was performed using Photoshop (Adobe).

Pharmacological treatment of cortical and hippocampal neurons. Cortical neurons (5 DIV) were starved in serum-free Neurobasal medium for 4–6 h at 37 °C before addition of BDNF (100 ng ml^{-1}) for the indicated duration. To examine dendritic spines of cultured hippocampal neurons, half of the medium was changed the day before BDNF treatment, and neurons (13 DIV) were treated with BDNF (100 ng ml^{-1}) for 24 h. To examine glutamate-induced PAK phosphorylation, cortical neurons (13 DIV) were silenced by tetrodotoxin (1 μM) and NBQX (10 μM) in MEM for 4 h before treatment with glutamate (50 μM) for 5 min. Stimulation of cortical neurons (14–16 DIV) by bicuculline (20 μM) and glycine (200 μM) was performed in Mg^{2+}-free buffer (140 mM NaCl, 1.3 mM $CaCl_2$, 5 mM KCl, 25 mM HEPES and 33 mM glucose) as previously described[30].

Glutamate uncaging and live cell imaging. Hippocampal neurons (2×10^5 neurons per dish) were seeded on 35-mm dishes with 18-mm central coverglasses (SPL Lifesciences) coated with poly-D-lysine (1 mg ml^{-1}). Neurons (10 DIV) were transfected with EmGFP by calcium phosphate precipitation. At 17–18 DIV, neurons were switched to the Mg^{2+}-free buffer described above and treated with MNI-glutamate (1 mM). Imaging was performed using a Nikon A1 scanning confocal microscope at 5% CO_2 and 37 °C using stage top incubator (Tokai Hit). Dendritic segments on basal dendrites of GFP-positive neurons were imaged by 60× oil-immersion objective with 4× optical zoom using the Galvano scanning mode, and eight to ten serial optical sections that covered ~4-μm depth of field were taken before glutamate uncaging. Photolysis of caged glutamate was performed by 405-nm laser (36 mW). A region of interest was selected in close proximity to the spine of interest. The region of interest was illuminated by four trains of laser at 1 Hz (7-μs pixel dwell time) using the Resonant scanning mode. The dendritic segment was then imaged using the Galvano scan mode (with the same acquisition setting before photolysis) over a period of 20 min. Image analyses were performed with Metamorph software (Meta image series 7.5, Universal Imaging). For quantification, the same dendritic spine before and at different times after glutamate uncaging was outlined after thresholding the background. The fold change in spine area (as compared with the one before glutamate uncaging) at the indicated time points after glutamate uncaging was measured.

Immunofluorescence staining, Golgi staining, image acquisition and quantitative analysis. To examine the localization of p-S478 TrkB and PSD-95, low density hippocampal neurons were fixed with 4% paraformaldehyde/4% sucrose (wt/vol) for 15 min, followed by blocking (0.4% Triton X-100 (vol/vol) and 1% BSA (vol/vol)) for 45 min, and incubated with antibodies to phospho-S478 TrkB (1:150) and PSD-95 (1:400) in blocking solution at 4 °C overnight. After washing three times with washing buffer (0.02% Triton X-100 and 0.25% BSA in PBS), neurons were incubated with Alexa Fluor–conjugated secondary antibodies (diluted in 0.02% Triton X-100 and 1% BSA in PBS) at 22–25 °C for 1 h, washed twice by the washing buffer, and mounted by hydromount (National Diagnostics). For co-staining of total TrkB and PSD-95, neurons were fixed with methanol at −20 °C for 15 min. Neurons were incubated with primary antibodies diluted in GDB buffer (30 mM phosphate buffer pH 7.4 containing 0.2% gelatin (by weight)), 0.5% Triton X-100 and 0.8 M NaCl) at 4 °C overnight. After washing three times with washing buffer (20 mM phosphate buffer and 0.5 M NaCl), neurons were incubated with secondary antibodies (diluted in GDB buffer) at 22–25 °C for 1 h, washed three times by the washing buffer, and mounted by hydromount. For TrkB surface staining, hippocampal neurons were incubated with the chicken antibody to TrkB (diluted in conditioned medium, 1:200) at 37 °C for 10 min. After a brief wash by PBS, neurons were immediately fixed by 4% paraformaldehyde/4% sucrose for 8 min. Neurons were incubated with Alexa Fluor–conjugated antibody to chicken (diluted in GDB buffer) for 1 h, after which cells were washed by washing buffer (20 mM phosphate buffer, 0.5 M NaCl) and PBS, and incubated with antibody to MAP2 at 4 °C overnight, followed by procedure as described above. For the double-staining of phospho-S478 TrkB and TIAM1, sequential staining with the two primary antibodies was performed, and the tyramide signal amplification kit (Invitrogen) was used to detect phospho-S478 TrkB.

Golgi impregnation was performed with the FD Rapid Golgistain Kit according to the manufacturer's instruction: *Trkb*$^{+/+}$ and *Trkb*$^{S478A/S478A}$ mice were killed at postnatal day 75. Half of the brains were immersed in solutions A and B for 5 d and incubated with solution C for 1 week. The brains were imbedded in distilled water and cut into 100-μm coronal sections using cryostat. Sections were mounted on gelatinized glass slides and processed for the Golgi staining procedure. Pyramidal neurons in hippocampal CA1 and CA3 regions were imaged for the quantification of dendritic arbors. Dendritic protrusions on the secondary branching from the apical dendrite of CA1 pyramidal neurons were quantified.

For image acquisition, images were acquired by a Nikon A1 confocal microscope with a 60× oil-immersion objective. We collected 8–12 serial individual optical sections (*z* interval of 0.4 μm). Images from the same experiment were obtained using identical acquisition settings. For imaging of dendritic spines in GFP-transfected hippocampal neurons, images were acquired by Olympus Fluoview FV1000 confocal microscope with a 60× oil-immersion objective using *z* serial scanning mode, and image analyses were performed with Metamorph software. For quantification, two to three dendrite segments from each neuron were analyzed. The basal threshold values for the background of all images in each experiment were measured. The average of these threshold values was then applied to all images in the same experiment.

Statistical analysis. Statistical analysis was performed, where appropriate, using Student's *t*-test or ANOVA followed by tests as indicated in the figure legends. Statistical significance of experiments involving two experimental conditions was assessed by unpaired Student's *t*-test (two-sided), whereas that of experiments involving three or more experimental conditions was assessed by one-way ANOVA followed by Tukey, Newman-Keuls or Bonferroni's *post-hoc* test. All experiments were performed at least three times except those specifically indicated.

51. Liu, P. *et al.* Bcl11a is essential for normal lymphoid development. *Nat. Immunol.* **4**, 525–532 (2003).
52. Southon, E. & Tessarollo, L. Manipulating mouse embryonic stem cells. *Methods Mol. Biol.* **530**, 165–185 (2009).
53. Reid, S.W. & Tessarollo, L. Isolation, microinjection and transfer of mouse blastocysts. *Methods Mol. Biol.* **530**, 269–285 (2009).
54. Xie, H. *et al.* Brain-derived neurotrophic factor rescues and prevents chronic intermittent hypoxia-induced impairment of hippocampal long-term synaptic plasticity. *Neurobiol. Dis.* **40**, 155–162 (2010).
55. Fu, W.Y. *et al.* Cdk5 regulates EphA4-mediated dendritic spine retraction through an ephexin1-dependent mechanism. *Nat. Neurosci.* **10**, 67–76 (2007).